



ELSEVIER

Physica B 272 (1999) 31–35

PHYSICA B

www.elsevier.com/locate/physb

# Microwave spectroscopy of a double quantum dot in the low- and high-power regime

W.G. van der Wiel<sup>a,b,\*</sup>, T. Fujisawa<sup>b</sup>, T.H. Oosterkamp<sup>a</sup>, L.P. Kouwenhoven<sup>a</sup>

<sup>a</sup>*Department of Applied Physics and Delft Institute of Microelectronics and Submicron-technology (DIMES), Delft University of Technology,  
PO Box 5046, 2600 GA Delft, The Netherlands*

<sup>b</sup>*NTT Basic Research Laboratories, 3-1, Morinosato Wakamiya, Atsugi-shi, Kanagawa 243-0198, Japan*

## Abstract

Microwave experiments on an artificial two-level system formed by a double quantum dot, are discussed for different coupling and microwave power regimes. When the inter-dot coupling,  $T$ , is weak, an ionic-like bonding is observed. The current through the double dot is power dependent. In the strong coupling regime, a covalent-like bonding is formed and the energy separation between the symmetric and anti-symmetric eigenstates,  $\Delta E^*$ , becomes power dependent as well. It is given by  $\Delta E^* = \sqrt{\{\Delta E\}^2 + \{2J_0(eV_{AC}/hf)T\}^2}$ , where  $\Delta E$  is the uncoupled energy splitting,  $J_0$  the zeroth-order Bessel function of the first kind,  $V_{AC}$  the microwave amplitude, and  $f$  the frequency. We show that in the case of strong coupling and low microwave power ( $eV_{AC} \ll hf, J_0 \approx 1$ ), the observed energy separation is well described by  $\Delta E^* = \sqrt{\{\Delta E\}^2 + \{2T\}^2}$ . For larger microwave powers ( $eV_{AC} \gtrsim hf$ ) it is shown that the energy separation is modified according to the Bessel function term. © 1999 Published by Elsevier Science B.V. All rights reserved.

*Keywords:* Two-level system; Double quantum dot; Mesoscopic physics

The fabrication of artificial tunable two-level systems in a solid-state environment allows the experimental study of fundamental quantum physics [1–5]. In addition to that, these systems obtain increasing interest, because of their possible application as quantum bits or ‘qubits’, the basic elements of a quantum computer [6]. A double quantum dot, a system of two quantum dots coupled to each other, can be used as such an artificial tunable two-level system. Quantum dots are small confined regions in a semiconductor, containing a variable number of electrons (from zero to

several hundreds) that occupy well-defined, discrete quantum states. Quantum dots are often referred to as artificial atoms because of their analogies with real atoms [7] and hence the name ‘artificial molecule’ for a double-dot system [5,8]. Depending on the strength of the inter-dot coupling, the two dots can form ionic-like [8–11] or covalent-like bonds [8]. In the first case, the electrons are localized on individual dots, while in the second case, the electrons are delocalized over both dots. The covalent binding leads to a symmetric and anti-symmetric state, whose energy difference is proportional to the degree of tunneling. Multiple-gated structures for the double dot allow us to independently control their energy levels, the coupling strength between the dots, as well as the tunneling rate to the leads.

\* Corresponding author. Fax: + 31-15-278-3251.

E-mail address: wilfred@qt.tn.tudelft.nl (W.G. van der Wiel)

A DC bias voltage and an AC (microwave) voltage can be used to modulate the electron occupation of the states. This controllability allows us to study the manipulation of quantum states for future quantum logic gates. In a superconducting system, non-adiabatic control of the states has been shown to create a coherent charge oscillation for a desired time [6]. Here, we present microwave experiments (0–50 GHz) on double quantum dots for different coupling and microwave power regimes. Both weakly coupled and strongly coupled dots in the low- and high-power microwave regime are discussed. For weakly coupled dots we show how the height of the main resonance and the current peaks associated with the absorption or emission of photons, are affected by high-power microwave irradiation. For strongly coupled dots it is shown how a high-power microwave field affects the energy difference between the symmetric and anti-symmetric states in the dots.

When the coupling between the two dots is weak, electrons are strongly localized on the individual dots. The gate voltages are used to surmount the single-electron charging energy and to align a discrete energy level in the left dot with a discrete energy level in the right dot [12]. Then, it is energetically allowed for an electron to tunnel between the dots. A current can flow when the two energy levels are aligned within the bias voltage window, defined by the electrochemical potentials of the left and right lead. Note that energy is also conserved when photons of energy  $hf$ , which match the energy difference between the states of the two dots, are absorbed from the microwave field. The possible tunnel processes are schematically depicted in Fig. 1a. The inset to Fig. 1b shows a SEM photograph of the double-dot device in which the source and drain regions and the double dot are indicated schematically [9]. The resonance in the lowest trace in Fig. 1a is due to an alignment of discrete energy levels. The other traces are measured while applying a microwave signal. The satellite resonances are due to photon assisted tunneling (PAT) processes which involve the emission (left satellite) or absorption (right satellite) of a microwave photon [13]. An AC voltage drop  $V = V_{AC} \cos(2\pi ft)$  ( $V_{AC}$  and  $f$  are the microwave amplitude and frequency, respectively) across

a tunnel barrier modifies the tunnel rate through the barrier as [14]

$$\Gamma^*(E) = \sum_{n=-\infty}^{\infty} J_n^2(\alpha) \Gamma(E + nhf). \quad (1)$$

Here,  $\Gamma^*(E)$  and  $\Gamma(E)$  are the tunnel rates at energy  $E$  with and without an AC voltage, respectively.  $J_n^2(\alpha)$  is the square of the  $n$ th-order Bessel function evaluated at  $\alpha = eV_{AC}/hf$ , which describes the probability that an electron absorbs or emits  $n$  photons of energy  $hf$ . The squared Bessel functions for  $n = 0, 1, 2$  are given in Fig. 1c. The inset schematically shows the first two photon side bands developed in the presence of a microwave field.

As the power is increased, satellite peaks appear corresponding to the absorption of multiple photons, which are observed up to  $n = 11$  [8]. A high-power microwave field strongly perturbs tunneling. This is reflected by the non-linear dependence of the peak heights on microwave power. In Fig. 1d, the peak heights of the main peak and the first two photon satellite peaks are shown, which agree well with the expected squared Bessel function behaviour as shown in Fig. 1c.

Fig. 1b shows that the energy separation of the satellite peaks from the main peak,  $\Delta E$ , depends linearly on frequency between 1 and 50 GHz. As we will discuss below, this linearity implies that the tunnel coupling is negligible. The electrons are localized on the individual dots and they have an ionic bonding. The line proportional to  $2hf$  is taken from data at higher microwave powers where electrons absorb or emit two photons during tunneling.

Our strong-coupling measurements were made on a second type of double-dot sample (see inset to Fig. 2b) [10]. To single out the current only due to microwaves we operate the device as an electron pump driven by photons in a way described theoretically in Refs. [15,16] (see the diagrams of Fig. 2a). When the two dots are strongly coupled, a symmetric and anti-symmetric eigenstate is formed. The energy separation between the symmetric and anti-symmetric eigenstates,  $\Delta E^*$ , is given by  $\Delta E^* = \sqrt{\{\Delta E\}^2 + \{2J_0(\alpha)T\}^2}$ , where  $\Delta E$  is the uncoupled energy splitting ( $\Delta E = E_{\text{left}} - E_{\text{right}}$ ) and  $T$  is the tunnel coupling between the two dots. When the sample is irradiated, an excitation may

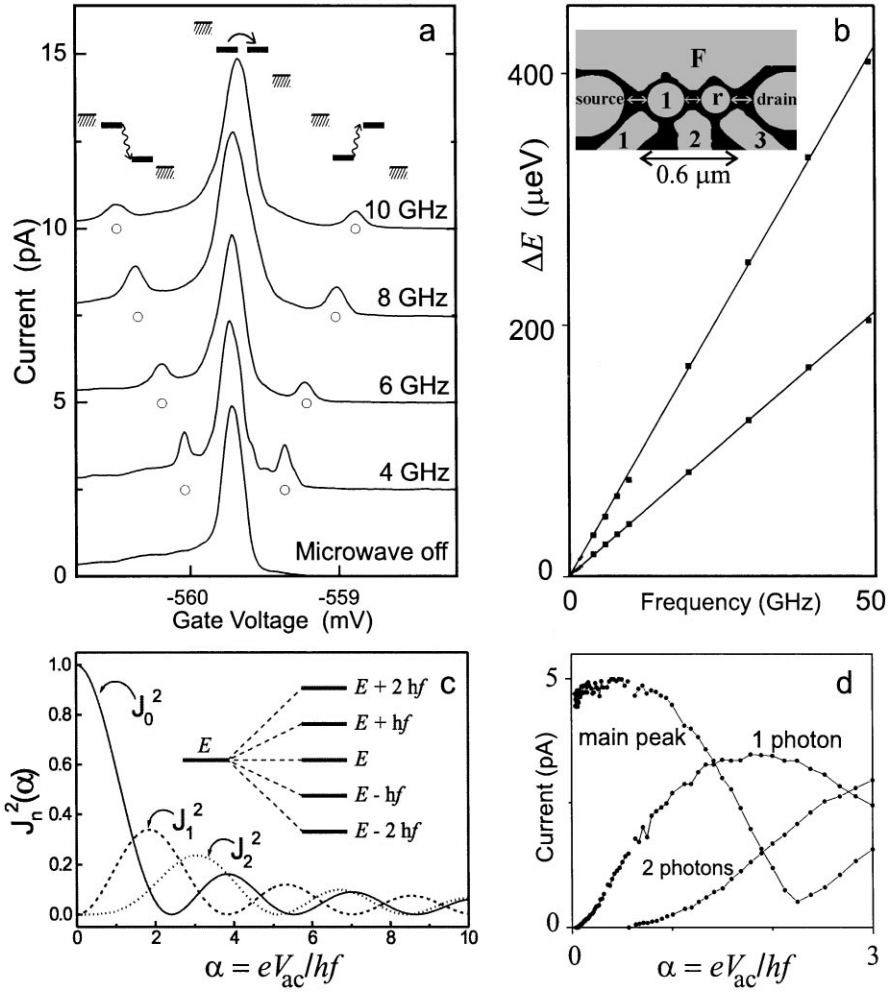


Fig. 1. Weakly coupled double quantum dot in the low- and high-power microwave regime. (a) The upper diagrams illustrate three situations of the energy state in the left dot relative to the state in the right dot. The hatched lines denote the Fermi levels in the leads. The bottom curve shows the current as a function of the voltage on gate 1 (see inset to Fig. 1b) for source-drain voltage,  $V_{SD} = 500 \mu\text{V}$  without applying microwaves. A single resonance occurs when two states line up. The other curves, which have been offset for clarity, show the current when microwaves with frequency  $f$  from 4 to 10 GHz are applied. Now, two additional satellite resonances occur when the two states are exactly a photon energy apart. The corresponding photon-assisted tunneling processes are illustrated in the upper diagrams. (b) Distance between the main resonance and the first two satellites as a function of the applied frequency from 1 to 50 GHz. The distance is transferred to energy through  $\Delta E = \kappa \Delta V_g$  where  $\kappa$  is the appropriate capacitance ratio for our device that converts gate voltage to energy [12]. The agreement between the data points and the two solid lines, which have slopes of  $h$  and  $2h$ , demonstrates that we observe the expected linear frequency dependence of the one and two photon processes. Inset, double quantum dot used for the presented measurements [9]. (c) Squared Bessel functions of the first kind,  $J_n^2(\alpha)$ , for  $n = 0, 1, 2$ . The inset schematically shows the development of sidebands of the original energy as a consequence of the microwave field. The population probability  $P(n)$  of the different sidebands is given by  $P(n) = J_n^2(eV_{AC}/hf)$ . A positive or negative  $n$  corresponds to the absorption or emission, respectively, of  $n$  photons during the tunnel process. Elastic tunneling corresponds to  $n = 0$ . (d) Height of the main peak and the first two satellite peaks as function of microwave power. The experimental height dependence agrees with the expected squared Bessel function behaviour as shown in (c).

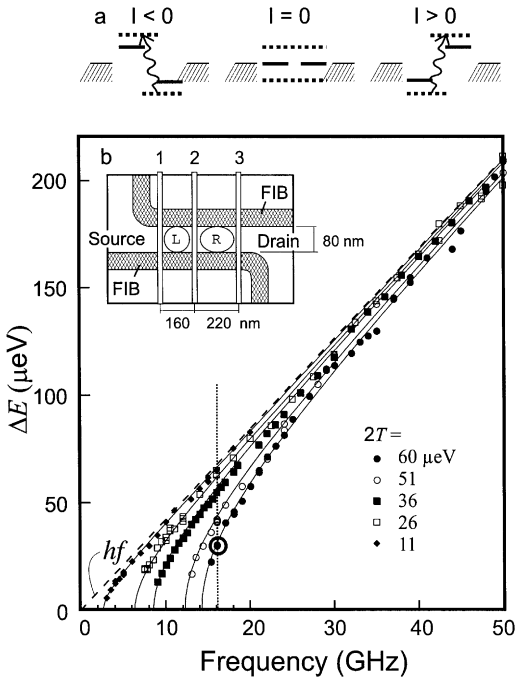


Fig. 2. Strongly coupled double dot in the low-power microwave regime. (a) Energy diagrams. Solid lines depict the energy states  $E_{\text{left}}$  and  $E_{\text{right}}$  in the two dots for the case that the coupling is weak and that their energy difference is simply  $\Delta E = E_{\text{left}} - E_{\text{right}}$ . When the dots are strongly coupled, the states delocalize over both dots thereby forming a symmetric and an anti-symmetric state. These are indicated by two dotted lines. Their energy difference is  $\Delta E^* = \sqrt{\{\Delta E\}^2 + \{2J_0(\alpha)T\}^2}$ . Electrons are transferred from the symmetric to the anti-symmetric state when  $\Delta E^* = hf$ . In the first diagram  $E_{\text{left}} > E_{\text{right}}$ , which results in electron pumping from right to left corresponding to a negative current. In the second diagram the whole system is symmetric  $E_{\text{left}} = E_{\text{right}}$  and consequently the net electron flow must be zero. In the third diagram  $E_{\text{left}} < E_{\text{right}}$ , which gives rise to pumping from left to right and a positive current. (b) Half the spacing in gate voltage between the positive and negative satellite peaks as a function of frequency. The microwave power is kept as low as possible in order to meet the condition  $eV_{\text{AC}} < hf$ . In that case  $J_0^2(\alpha) \approx 1$  and the relation  $\Delta E = \sqrt{\{hf\}^2 - \{2T\}^2}$  is expected to be valid. Gate voltage spacing has been transferred to energy difference  $\Delta E$  (see also figure caption 1b). Different curves correspond to different coupling constants  $T$ . The solid lines are theoretical fits to  $\Delta E = \sqrt{\{hf\}^2 - \{2T\}^2}$ . In the limit of weak coupling, this reduces to  $\Delta E = hf$ , which is indicated by the dashed line. The resulting values for  $2T$  are given in the figure. The coupling is varied by applying different voltages to the centre gate (2) or by changing the magnetic field ( $\blacklozenge$ )  $B = 3.3$  T; ( $\blacksquare$ )  $B = 2.2$  T; other curves  $B = 0$  T). The upper left inset shows a diagram of the sample [10]. A narrow channel is defined by locally depleting the 2DEG using focussed ion beam (FIB) implantation. Applying negative voltages to the three gates (1–3)

result as illustrated in Fig. 2a. A non-zero current indicates that an electron is excited from the symmetric to the anti-symmetric state, thereby fulfilling the condition  $hf = \Delta E^*$ , or conversely

$$\Delta E = \sqrt{\{hf\}^2 - \{2J_0(\alpha)T\}^2}. \quad (2)$$

The coupling between the dots can be decreased by changing the gate voltage on the centre gate to more negative values or by applying a magnetic field perpendicular to the sample. In Fig. 2b, we have plotted the energy spacing  $\Delta E$  at which the pumping current is at a maximum, as a function of frequency. The microwave power is kept as low as possible in order to meet the condition  $eV_{\text{AC}} \ll hf$ . In that case,  $J_0^2(\alpha) \approx 1$  and the relation

$$\Delta E = \sqrt{\{hf\}^2 - \{2T\}^2}, \quad (3)$$

is expected to be valid. Different labels correspond to different centre gate voltage settings and magnetic fields. The solid lines are fits of Eq. (3) to the measured data. It follows that the coupling  $2T$  has been tuned from 11 to 60  $\mu\text{eV}$ . The good agreement with Eq. (3) demonstrates the control over the formation of a covalent bonding between the two dots and that the condition  $eV_{\text{AC}} \ll hf$  has been satisfied.

We now discuss the case  $eV_{\text{AC}} \gtrsim hf$ . As can be seen in Fig. 1c,  $J_0^2(\alpha)$  deviates from 1 in this case and cannot be neglected as before. We discuss below a coupling of 60  $\mu\text{eV}$  and a microwave frequency of 16 GHz, as indicated by the circle in Fig. 2b. Similar results have been obtained for other couplings and microwave frequencies. The inset to Fig. 3 shows the measured PAT current as a function of  $\Delta E$  for different powers. The absolute value of the microwave power at the position of the double quantum dot is unknown. Therefore, we use a relative microwave power scale, which is expressed in terms of the attenuation of the microwave source signal in units dB. The positions of the PAT peaks at the lowest power are indicated with two dashed

that cross the channel then forms two dots. Microwaves are capacitively coupled to gate 2. The open black circle marks a coupling of 60  $\mu\text{eV}$  and frequency of 16 GHz (dotted line), which are the conditions used for the high-power results shown in Fig. 3.

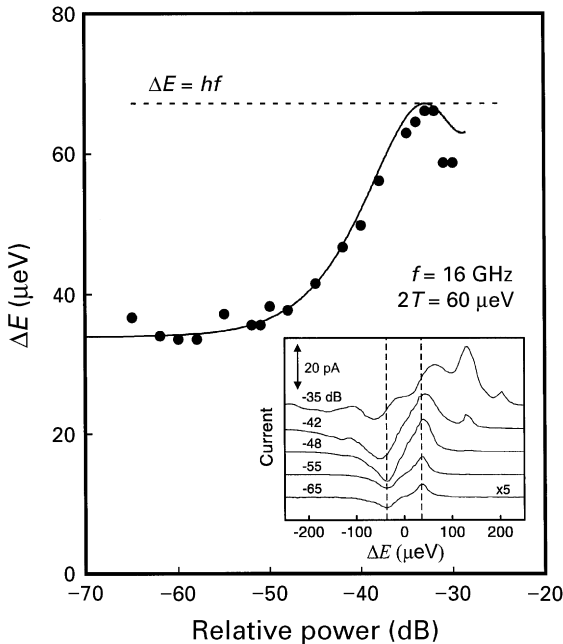


Fig. 3. Strongly coupled double dot ( $2T = 60 \mu\text{eV}$ ) in the high-power microwave regime for  $f = 16 \text{ GHz}$ . The inset shows the measured PAT current as a function of  $\Delta E$  for different powers. We use a relative microwave power scale, which is expressed in terms of the attenuation of the microwave source signal in units dB. The positions of the PAT peaks at the lowest power are indicated with two dashed lines. Increasing the microwave power from the lowest value, the PAT peak separation becomes larger. For higher powers, multiple-photon processes can take place, which result in extra current peaks. Additional structure in the high-power current measurements can also be caused by photon-assisted pumping [17], which is due to an asymmetric AC voltage drop across the double dot. In the main part, half the PAT peak separation energy as a function of the relative microwave power is shown. The solid line is a fit to  $\Delta E = \sqrt{\{hf\}^2 - \{2J_0(\alpha)T\}^2}$ ,  $f = 16 \text{ GHz}$ ,  $2T = 60 \mu\text{eV}$ . Because of the relative power scale, the fitting curve has been adjusted horizontally to obtain the best fit.

lines. Increasing the microwave power from the lowest value, the PAT peak separation becomes larger, which is in agreement with Eq. (2). For higher powers, multiple-photon processes can take place, which result in extra current peaks. Additional structure in the high-power current measurements can also be caused by photon-assisted pumping [17], which is due to an asymmetric AC voltage drop across the double dot. The main part of Fig. 3 shows half the PAT peak separation energy as a function of the relative microwave power.

The solid line is a fit with Eq. (2),  $f = 16 \text{ GHz}$ ,  $2T = 60 \mu\text{eV}$ . Because of the relative power scale, the fitting curve has been adjusted horizontally to give the best fit. The microwave power effectively reduces the coupling between the dots. This is illustrated by the vertical dotted line in Fig. 2b at  $f = 16 \text{ GHz}$ . At  $-33 \text{ dB}$  the energy separation equals  $hf$ , which implies that the effective coupling is zero. This means  $J_0^2(\alpha)$  has its first zero and  $\alpha = eV_{\text{AC}}/hf = 2.4$  and hence  $V_{\text{AC}} = 0.16 \text{ mV}$ . This provides an estimate for the absolute power applied to the device.

We discussed microwave spectroscopy on weakly and strongly coupled dots, applying both low and high powers of microwave radiation. Our results agree well with theory and form an encouraging basis for future study of double quantum dot devices. Time-resolved measurements and study of decoherence phenomena will play a role of central interest.

## Acknowledgements

L.P.K. acknowledges financial support from the Dutch Organization for Fundamental Research on Mater (FOM), from the NEDO joint research program (NTDP-98), and from the EU via a TMR network.

## References

- [1] K. Leo et al., Phys. Rev. Lett. 66 (1991) 201.
- [2] E.E. Mendez, G. Bastard, Phys. Today 46 (1993) 34.
- [3] D.J. Flesch et al., Phys. Rev. Lett. 78 (1997) 4817.
- [4] Y. Nakamura et al., Phys. Rev. Lett. 79 (1997) 2328.
- [5] G. Schedelbeck et al., Science 278 (1997) 1792.
- [6] Y. Nakamura et al., Nature 398 (1999) 786.
- [7] R. Ashoori, Nature 379 (1996) 413.
- [8] T.H. Oosterkamp et al., Nature 395 (1998) 873.
- [9] N.C. van der Vaart et al., Phys. Rev. Lett. 74 (1995) 4702.
- [10] T. Fujisawa, S. Tarucha, Superlatt. Microstruct. 21 (1997) 247.
- [11] T. Fujisawa, S. Tarucha, Jpn. J. Appl. Phys. 36 (1997) 4000.
- [12] L.P. Kouwenhoven et al., in: L. Sohn et al. (Eds.), Electron Transport in Quantum Dots in Mesoscopic Electron Transport, Serves E, Kluwer, Dordrecht, 1997, pp. 105–214, see also <http://vortex.tn.tudelft.nl/leok/papers>.
- [13] T.H. Stoof, Yu.V. Nazarov, Phys. Rev. B 53 (1996) 1050.
- [14] P.K. Tien, J.R. Gordon, Phys. Rev. 129 (1963) 647.
- [15] C.A. Stafford, N.S. Wingreen, Phys. Rev. Lett. 76 (1996) 1916.
- [16] Ph. Brune et al., Physica E 1 (1997) 216.
- [17] T.H. Oosterkamp et al., cond-mat/9904359, 1999.